IHEP 2004-12

High statistic measurement of the $K^- \to \pi^0 e^- \nu$ decay form-factors

O.P. Yushchenko, S.A. Akimenko, G.I. Britvich, K.V.Datsko, A.P. Filin, A.V. Inyakin, A.S. Konstantinov, V.F. Konstantinov, I.Y. Korolkov, V.A. Khmelnikov, V.M. Leontiev, V.P. Novikov, V.F. Obraztsov, V.A. Polyakov, V.I. Romanovsky, V.M. Ronjin, V.I. Shelikhov, N.E. Smirnov[1], O.G. Tchikilev, V.A.Uvarov.

Institute for High Energy Physics, Protvino, Russia

V.N. Bolotov, S.V. Laptev, A.Yu. Polyarush.

Institute for Nuclear Research, Moscow, Russia

Abstract

The decay $K^- \to \pi^0 e^- \nu$ is studied using in-flight decays detected with the "ISTRA+" spectrometer. About 920K events are collected for the analysis. The λ_+ slope parameter of the decay form-factor $f_+(t)$ in the linear approximation (average slope) is measured: $\lambda_+^{\rm lin} = 0.02774 \pm 0.00047(\rm stat) \pm 0.00032(\rm syst)$. The quadratic contribution to the form-factor was estimated to be $\lambda_+^{'} = 0.00084 \pm 0.00027(\rm stat) \pm 0.00031(\rm syst)$. The linear slope, which has a meaning of $df_+(t)/dt|_{t=0}$ for this fit, is $\lambda_+ = 0.02324 \pm 0.00152(\rm stat) \pm 0.00032(\rm syst)$. The limits on possible tensor and scalar couplings are derived: $f_T/f_+(0) = -0.012 \pm 0.021(\rm stat) \pm 0.011(\rm syst)$, $f_S/f_+(0) = -0.0037^{+0.0066}_{-0.0056}(\rm stat) \pm 0.0041(\rm syst)$.

[1]Now at INFN, Padova, Italy

1 Introduction

The decay $K \to e\nu\pi$ (K_{e3}) provides unique information about the dynamics of the strong interactions. It has been a testing ground for such theories as current algebra, PCAC, Chiral Perturbation Theory(ChPT). The study of this decay has a particular interest in view of new two-loop order ($O(p^6)$) calculations for K_{l3} decays in ChPT [1, 2].

The high-order ChPT calculations make a definite prediction for the quadratic term in the vector ($f_+(t)$) form-factor and link the scalar ($f_0(t)$) form-factor linear and quadratic slopes to the $f_+(0)$ corrections. In turn, $f_+(0)$ is known to be crucial for the $|V_{us}|$ measurements. In fact, the latest measurements do not report any visible non-linearity in the form-factors [3, 4, 5, 6].

In this paper we present a high-statistics measurement ($\sim$ 919K events) of the Dalitz plot density in this decay. The description of the experimental setup, trigger and reconstruction procedure can be found in our previous paper [5].

2 Selection procedure

The current analysis is based on the high-statistics data collected during run in Winter 2001. In total, 332M events were logged on tapes. This statistics is complemented by about 160M MC events generated with Geant3 [7] Monte Carlo program. The MC generation includes a realistic description of the setup with decay volume entrance windows, tracking chambers windows, chambers gas mixtures, sense wires and cathode structures, Čerenkov counters mirrors and gas, the shower generation in EM calorimeters, etc.

The events with one charged track identified as electron and two or three additional showers in the electromagnetic calorimeter are selected for further processing.

It was observed, that the main background contribution (about 95% of the background events) is related to the decay $K^- \to \pi^-\pi^0$, when the hadronic interaction of the charged pion simulates the electromagnetic shower in the calorimeter. Following the method of angular selection used in our analysis of the $K_{\mu3}$ decay [6], we choose the angle between the beam particle direction and the vector sum of momenta of the final state track and photons as the variable to perform signal-background separation.

The expected distribution over this angle is shown in Fig.1 together with the real data. One can observe a clear background peak at small values and a good agreement of the data and Monte-Carlo. The cut value was selected in the region where the maximum of the function $\mathrm{Eff}_{\mathrm{Signal}}/\mathrm{Eff}_{\mathrm{Back.}}$ is reached.

After that, the momenta of the final state particles were refined with 2C $K \to e\nu\pi^0$ kinematic fit. Only the convergence of the fit was required. The missing energy $E_\nu = E_K - E_\mu - E_{\pi^0}$ after 2C fit is shown in Fig.2. This variable should exhibit a strong peak at $E_\nu \sim 0$ in the presence of noticeable background contributions. The complete absence of any enhancement at small values of the missing energy proofs the quality of the selection procedure.

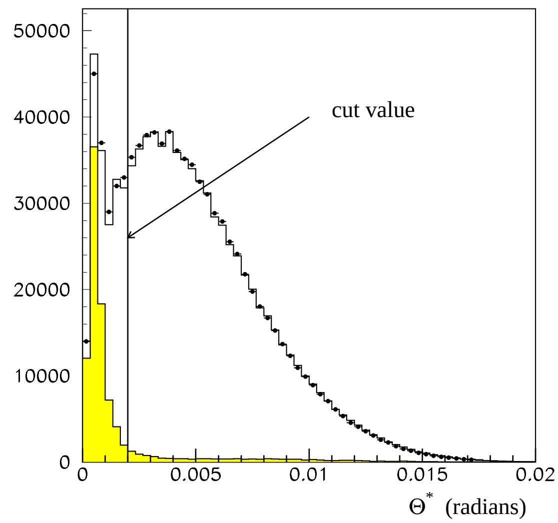

Figure 1: Angle between the beam track and the vector sum of final state particles momenta. The points with errors are data and the solid histogram is MC. The shaded area shows the background contribution.

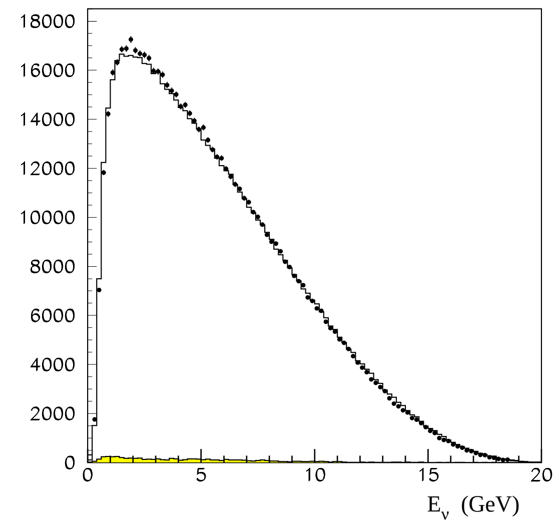

Figure 2: Energy of the neutrino compared with MC. The shaded area shows the surviving background contribution.

The signal Monte-Carlo events for Figures 1 and 2 are weighted with the K_{e3} matrix element where we use $\lambda_+ = 0.0286$ (fixed from our preliminary measurements [5]).

Finally, 919K events were selected. We estimate the surviving background contribution to be around 2.1%.

3 Analysis

The most general Lorentz-invariant form of the matrix element for the $K^- \to l^- \nu \pi^0$ decay is [8]:

$$M = \frac{G_F V_{us}}{2} \bar{u}(p_\nu)(1+\gamma^5)[2m_K f_S - [(P_K+P_\pi)_\alpha f_+ + (P_K-P_\pi)_\alpha f_-]\gamma^\alpha + i\frac{2f_T}{m_K}\sigma_{\alpha\beta} P_K^\alpha P_\pi^\beta] v(p_l) \quad (1)$$

It consists of scalar, vector, and tensor terms. The $f_\pm$ form-factors are the functions of $t = (P_K - P_\pi)^2$. In the Standard Model (SM), the W-boson exchange leads to the pure vector term. The scalar and/or tensor terms which are "induced" by EW radiative corrections are negligibly small, i.e nonzero scalar or tensor form-factors would indicate the physics beyond the SM.

The term in the vector part, proportional to f_-, is reduced (using the Dirac equation) to the scalar form-factor. In the same way, the tensor term is reduced to a mixture of the scalar and vector form-factors. The redefined vector (V) and scalar (S) terms, and the corresponding

Dalitz plot density in the kaon rest frame ($\rho(E_\pi, E_l)$) are [9]:

$$\begin{aligned}
\rho(E_\pi, E_l) &\sim A\cdot|V|^2 + B\cdot Re(V^*S) + C\cdot|S|^2 \\
V &= f_+ + (m_l/m_K)f_T \\
S &= f_S + (m_l/2m_K)f_- + \left(1+\frac{m_l^2}{2m_K^2} - \frac{2E_l}{m_K} - \frac{E_\pi}{m_K}\right) f_T \\
A &= m_K(2E_lE_\nu - m_K\Delta E_\pi) - m_l^2(E_\nu - \frac{1}{4}\Delta E_\pi) \\
B &= m_l m_K(2E_\nu - \Delta E_\pi);\ E_\nu = m_K - E_l - E_\pi \\
C &= m_K^2\Delta E_\pi;\ \Delta E_\pi = E_\pi^{max} - E_\pi;\ E_\pi^{max} = \frac{m_K^2 - m_l^2 + m_\pi^2}{2m_K}
\end{aligned} \tag{2}$$

With the selected number of events we can not neglect the $V-S$ interference term proportional to the electron mass. The term proportional to f_- is neglected in our analysis.

For further analysis we assume a general quadratic dependence of f_+ on t:

$$f_+(t) = f_+(0)\left(1 + \lambda_+ t/m_\pi^2 + \lambda_+^{'} t^2/m_\pi^4\right). \tag{3}$$

The procedure of the extraction of the form-factor parameters starts with the subdivision of the Dalitz plot region $y = 0.12 \div 0.92$; $z = 0.55 \div 1.075$ ($y = 2E_e/m_K,\ z = 2E_\pi/m_K$) into 100×100 bins.

The signal MC was generated with the constant matrix element and the amplitude-induced weights should be calculated during the fit procedure. One can observe that the Dalitz-plot density function $\rho(y,z)$ in (2) can be presented in the factorisable form:

$$\rho(y,z) = \sum_\alpha F_\alpha(\lambda_+, \lambda_+^{'}, f_S, f_T)\cdot K_\alpha(y,z), \tag{4}$$

where F_α are simple bilinear functions of the form-factor parameters and $K_\alpha(y,z)$ are the kinematic functions which are calculated from the MC-truth information. For each α, the sums of $K_\alpha(y,z)$ over events are accumulated in the Dalitz plot bins (i,j) to which the MC events fall after the reconstruction. Finally, every bin in the Dalitz plot gets weights $W_\alpha(i,j)$ and the density function $r(i,j)$ which enters into the fitting procedure is constructed:

$$r(i,j) = \sum_\alpha F_\alpha(\lambda_+, \lambda_+^{'}, f_S, f_T)\cdot W_\alpha(i,j) \tag{5}$$

This method allows one to avoid the systematic errors due to the "migration" of the events over the Dalitz plot due to the finite experimental resolution and automatically takes into account the efficiency of the reconstruction and selection procedures.

To take into account the finite number of MC events in the particular bin and strong variation of the real data events over the Dalitz plot, we minimize a $-\mathcal{L}$ function defined as [10]:

$$-\mathcal{L} = 2\sum_j n_j \ln\left[\frac{n_j}{r_j}\left(1 - \frac{1}{m_j+1}\right)\right] + 2\sum_j (n_j + m_j + 1)\ln\left(\frac{1+\frac{r_j}{m_j}}{1+\frac{n_j}{m_j+1}}\right), \tag{6}$$

where the sum runs over all populated bins, and n_j, r_j and m_j are the number of data events, expected events and generated Monte Carlo events respectively. For large m_j Eq. (8) reduces to the more familiar expression

$$-\mathcal{L} = \sum_j [2(r_j - n_j) + 2n_j \ln n_j / r_j]$$

The radiative corrections were taken into account by re-weighting every Monte-Carlo event, using MC-truth information, according to the recent calculations in [11].

The minimization is performed by means of the "MINUIT" program [12]. The errors are calculated by "MINOS" procedure of "MINUIT" at the level $\Delta\mathcal{L} = 1$, corresponding to 68% coverage probability for 1 parameter.

4 Results

A fit of the K_{e3} data with $f_S = f_T = \lambda'_+ = 0$ gives $\lambda_+ = 0.02774 \pm 0.00047$. The total number of bins is 6991 and $\chi^2/\text{ndf} = 0.97$. The quality of the fit is illustrated in figures 3 and 4 where the projected variables $y = 2E_e/m_K$ and $z = 2E_{\pi^0}/m_K$ are presented.

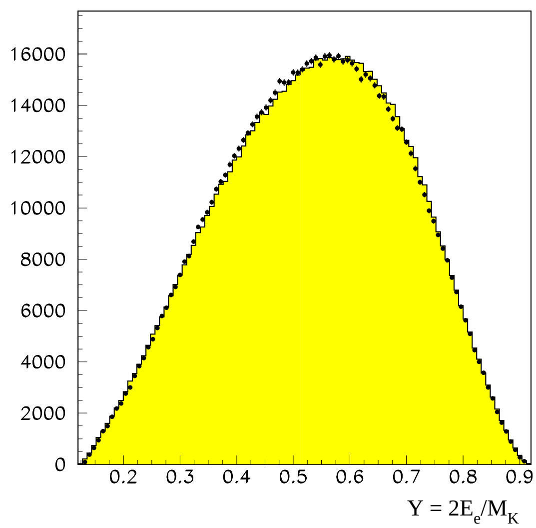

Figure 3: Y distribution.
The points with errors are the real data
and the shaded area – signal MC.

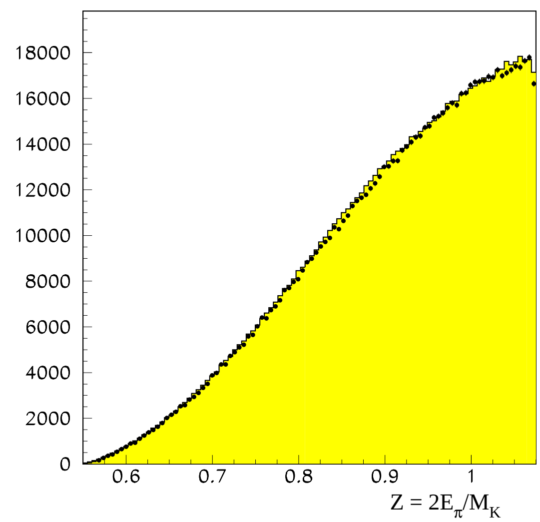

Figure 4: Z distribution.
The points with errors are the real data
and the shaded area – signal MC.

The Table 1 represents fits with possible nonlinear term in f_+ (Eq. 3) as well as the fits with tensor and scalar contributions (Eq. 1).

Every row of the Table 1 represents a particular fit where the parameters shown without errors are fixed. To qualify the statistical significance of the particular fit, we also show the change in the χ^2 value obtained with respect to the fit without non-linear or anomalous contributions.

The second row shows a fit where the nonlinearity is allowed in $f_+(t)$. One can observe $\lambda_+ - \lambda'_+$ (Fig.5) correlation that results in a significant λ_+ errors enhancement and visible shift of λ_+ parameter.

λ_+	λ'_+	$f_T/f_+(0)$	$f_S/f_+(0)$	$\Delta\chi^2$
0.02774 ± 0.00047	0.	0.	0.	0.
0.02324 ± 0.00152	0.00084 ± 0.00027	0.	0.	-9.8
0.02774 ± 0.00047	0.	-0.012 ± 0.021	0.	-0.3
0.02771 ± 0.00047	0.	0.	$-0.0059^{+0.0089}_{-0.0054}$	-0.5
0.02324 ± 0.00152	0.00084 ± 0.00027	-0.012 ± 0.021	0.	-9.9
0.02325 ± 0.00152	0.00084 ± 0.00027	0.	$-0.0037^{+0.0066}_{-0.0056}$	-9.9

Table 1. The K_{e3} fits.

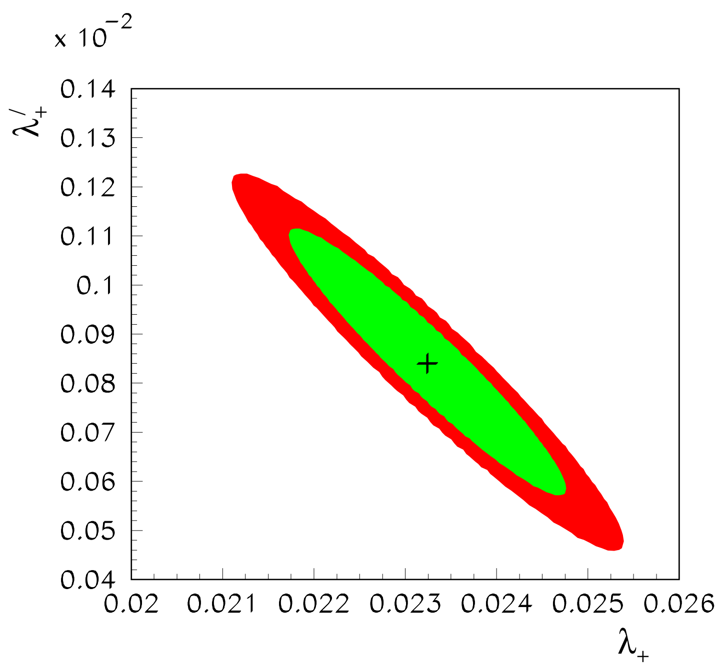

Figure 5: 1σ and 2σ contours in the $\lambda_+ - \lambda'_+$ plane.

. We should consider the λ_+ parameter in the linear approximation as a mean slope over all the physical q^2-region, while the true value of the linear slope $(df_+(t)/dt|_{t=0})$ should be taken from the non-linear fit.

We also perform model-independent one-dimensional (y) fits where the data in every of the 100 q^2/m_π^2 bins were fitted independently. The resulting distribution is shown in Fig.6. The normalization $f_+(0) = 1$ is assumed. The visible non-linearity can be observed in Fig.7, where the ratio $f_+(t)/f_+(0)/(1 + \lambda_+ q^2/m_\pi^2)$ is presented. The parabolic curve represents the fit with the quadratic non-linearity in the form-factor.

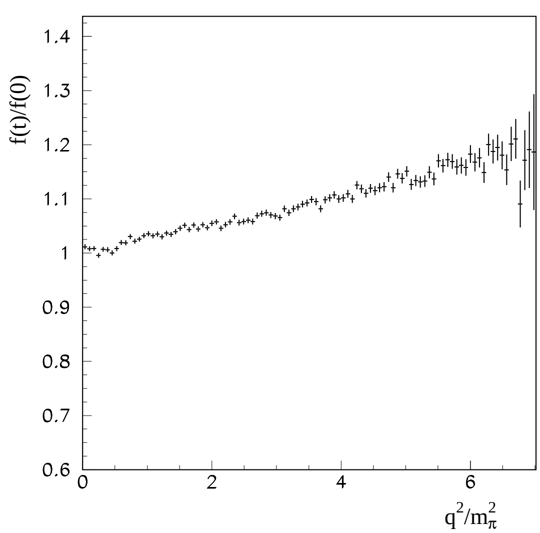

Figure 6: The value of $f_+(t)/f_+(0)$ obtained in the model-independent fits.

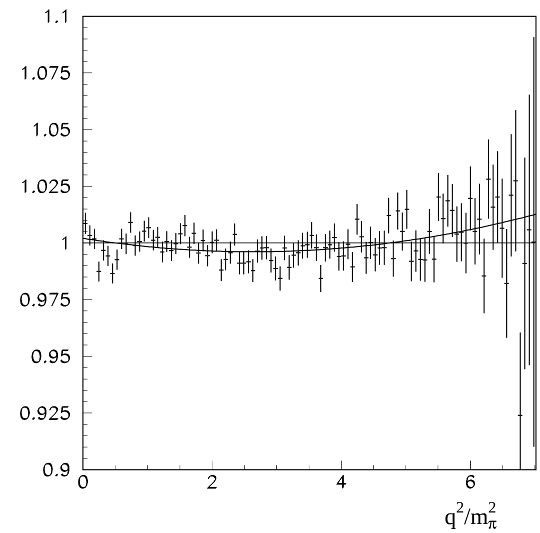

Figure 7: The value of $f_+(t)/f_+(0)/(1 + \lambda_+ q^2/m_\pi^2)$. The fit with non-linear contribution is shown.

This non-linearity can not be explained by a possible scalar contribution (that also results in the enhancement of the number of events at large values of q^2). The row 4 of the Table 1 represents a search for the scalar term with the vector form-factor set to be linear. The resulting value of $f_S/f_+(0)$ is compatible with zero.

We also perform a model-independent fit to extract simultaneously $f_+(t)$ and $f_S(t)$. The resulting distribution for the value $f_S(t)/f_+(0)$ is shown in Fig.8. The value of the scalar contribution is compatible with zero with strong enhancement of the errors at small values of t. This enhancement is explained by the dependence of the scalar contributions (Eq. 2) on the Dalitz variables. One can observe that the leading term $|S|^2$ is proportional to t and vanishes at $t \to 0$.

The last row of the Table 1 represents a fit with both scalar contribution and the quadratic term in the vector form-factor.

We also do not see any tensor contribution in our data (rows 3 and 5 in the Table 1).

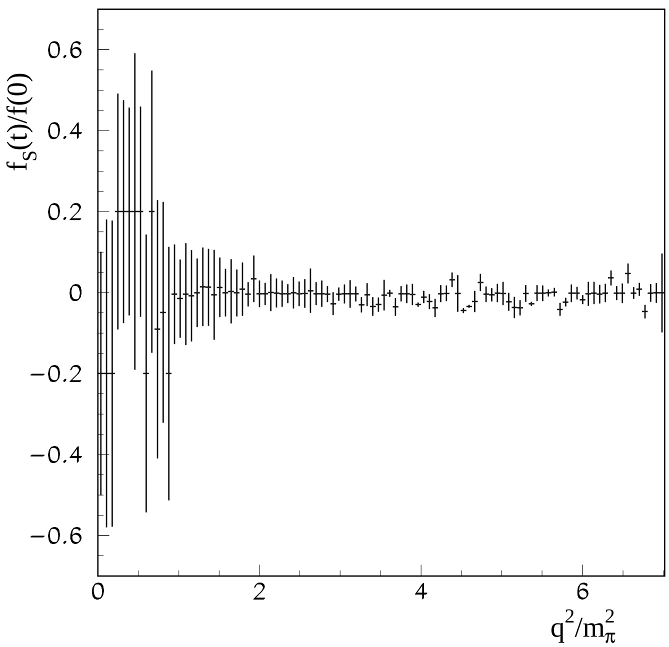

Figure 8: The value of $f_S(t)/f_+(0)$ obtained in the model-independent fit.

Different sources of systematics are investigated. We allow variations of the electron selection cuts and angular cut. The Dalitz plot binning, signal and background MC variations are also applied.

The systematic errors are summarized in the Table 2. We can conclude that the main contribution into systematic error comes from the main selection cut variation and from the limited amount of the background MC.

Source	λ_+	λ'_+	$f_T/f_+(0)$	$f_S/f_+(0)$
e^- selection	0.00017	0.00013	0.005	0.0020
angular cut	0.00020	0.00021	0.006	0.0020
Dalitz plot binning	0.00004	0.00006	0.001	0.0005
Signal MC variation	0.00006	0.00004	0.002	0.0006
Backg. MC variation	0.00016	0.00018	0.008	0.0026
Total	0.00032	0.00031	0.011	0.0041

Table 2. The systematic error contributions.

5 Summary and conclusions

The K^-_{e3} decay has been studied using in-flight decays of 25 GeV K^- detected by the "ISTRA+" magnetic spectrometer.

The λ_+ parameter of the vector form-factor in the linear approximation (average slope) is measured to be:

$$\lambda_+^{\rm lin} = 0.02774 \pm 0.00047\ (stat) \pm 0.00032\ (syst).$$

A visible non-linear contribution is observed for the first time :

$$\lambda'_+ = 0.00084 \pm 0.00027\ (stat) \pm 0.00031\ (syst).$$

With the quadratic term in the vector form-factor the linear slope (which has a meaning of $df_+(t)/dt|_{t=0}$) is determined to be:

$$\lambda_+ = 0.02324 \pm 0.00152\ (stat) \pm 0.00032\ (syst).$$

The limits on possible tensor and scalar couplings are derived from the fit with quadratic vector form-factor:

$$f_T/f_+(0) = -0.012 \pm 0.021\ (stat) \pm 0.011\ (syst);$$
$$f_S/f_+(0) = -0.0037^{+0.0066}_{-0.0056}\ (stat) \pm 0.0041\ (syst).$$

The value of the quadratic term in the vector form-factor is in a good agreement (within the statistical errors) with the O(p^6) ChPT predictions [1, 2].

The obtained limits on the scalar and tensor terms can be used to get limits on several exotic models.

The leptoquark-induced amplitudes for K_{e3} decay were considered in [13]. In this model the relation between tensor and scalar terms is fixed: $f_T = -6.87 f_S$. The fit of our data with this constraint gives the following scalar contribution: $f_S/f_+(0) = 0.0046^{+0.0042}_{-0.0067}$. This result can be converted in the upper limit $|f_S/f_+(0)| < 0.011$ (90% C.L.). Using the expression in [13]:

$$\frac{f_S}{f_+(0)} = \frac{\sqrt{2}}{16 G_F |V_{su}|} \frac{m_K^2 - m_\pi^2}{(m_s - m_u) m_K} \frac{1}{\Lambda_{LQ}^2}, \tag{7}$$

where Λ_{LQ} is the ratio of leptoquark mass to the square of the Yukawa-like coupling, we get

$$\Lambda_{LQ} > 2.55 \text{ TeV (90\% C.L.)}$$

Acknowledgments

We would like to thank Vincenzo Cirigliano for providing us with the program for the radiative correction calculations.

The work is supported by the RFBR grant N03-02-16330.

References

[1] P.Post and K.Schilcher, Eur. Phys. J. **25**(2002), 427.

[2] J.Bijnens and P.Talavera, Nucl.Phys. **B669**(2003), 341.

[3] S. Shimizu et al. (E246 KEK-PS Collaboration), Phys. Lett. **B495**(2000), 33.

[4] A.S. Levchenko et al. (E246 KEK-PS Collaboration), Yad.Fiz **v65**(2002), 2294,

[5] I.V.Ajinenko et al. (ISTRA+ Collaboration), Phys.Lett. **B574**(2003), 14.

[6] O.P.Yushchenko et al. (ISTRA+ Collaboration), Phys.Lett. **B581**(2004), 31.

[7] R Brun et al., CERN-DD/EE/84-1.

[8] H. Steiner et al., Phys.Lett. **B36**(1971), 521.

[9] M.V. Chizhov, Phys.Lett. **B381**(1996), 359.

[10] L. Rosselet et al., Phys.Rev. **D15**(1977), 574.

[11] V. Cirigliano, M. Knecht, H. Neufeld, H. Rupertsberger, P. Talavera, Eur. Phys. J. **C23**(2002), 121.

[12] F. James, M.Roos, CERN D506,1989.

[13] V.V. Kiselev, A.K. Likhoded and V.F. Obraztsov, hep-ph/0204066 (2002).